THE JOURNAL OF BIOLOGICAL CHEMISTRY
Vol. 276, No. 33, Issue of August 17, pp. 31193–31201, 2001
Printed in U.S.A.


# Coupled Electron/Proton Transfer in Complex Flavoproteins

## SOLVENT KINETIC ISOTOPE EFFECT STUDIES OF ELECTRON TRANSFER IN XANTHINE OXIDASE AND TRIMETHYLAMINE DEHYDROGENASE*

Received for publication, January 24, 2001, and in revised form, June 5, 2001
Published, JBC Papers in Press, June 6, 2001, DOI 10.1074/jbc.M100673200

**Russ Hille‡§ and Robert F. Anderson¶**

*From the ‡Department of Molecular and Cellular Biochemistry, Ohio State University, Columbus, Ohio 43210-1218 and the ¶Department of Chemistry, University of Auckland, Private Bag 92019, Auckland, New Zealand*

**A solvent kinetic isotope effect study of electron transfer in two complex flavoproteins, xanthine oxidase and trimethylamine dehydrogenase, has been undertaken. With xanthine oxidase, electron transfer from the molybdenum center to the proximal iron-sulfur center of the enzyme occurs with a modest solvent kinetic isotope effect of 2.2, indicating that electron transfer out of the molybdenum center is at least partially coupled to deprotonation of the Mo(V) donor. A Marcus-type analysis yields a decay factor, $\beta$, of 1.4 $Å^{-1}$, indicating that, although the pyranopterin cofactor of the molybdenum center forms a nearly contiguous covalent bridge from the molybdenum atom to the proximal iron-sulfur center of the enzyme, it affords no exceptionally effective mode of electron transfer between the two centers. For trimethylamine dehydrogenase, rates of electron equilibration between the flavin and iron-sulfur center of the one-electron reduced enzyme have been determined, complementing previous studies of electron transfer in the two-electron reduced form. The results indicate a substantial solvent kinetic isotope effect of 10 ± 4, consistent with a model for electron transfer that involves discrete protonation/deprotonation and electron transfer steps. This contrasts to the behavior seen with xanthine oxidase, and the basis for this difference is discussed in the context of the structures for the two proteins and the ionization properties of their flavin sites. With xanthine oxidase, a rationale is presented as to why it is desirable in certain cases that the physical layout of redox-active sites not be uniformly increasing in reduction potential in the direction of physiological electron transfer.**

Electron transfer in biological systems is often linked either directly or indirectly to protonation/deprotonation events, and the overall process may involve either discrete or concerted electron and proton transfer (1, 2). Coupled electron/proton transfer may occur in systems consisting of either organic species (*e.g.* quinones and flavins) or metal centers (as a result of protonation of ligands to the metal upon reduction). These effects are manifested in the pH dependence of the reduction potential(s) and may also influence the kinetics of electron transfer (1, 2). The uptake of protons with reduction of a metal center is an example of the principle of charge neutrality in biological systems, in which the protein environment of a redox-active center is thought to stabilize a given overall charge for a redox-active center, regardless of the specific oxidation state of the center.

We have previously examined electron transfer in complex redox-active enzymes using both pH jump and pulse radiolysis methodologies (3–9). Using the pH jump protocol, enzyme is placed in dilute buffer at a given pH and partially reduced by titration with a reagent such as sodium dithionite. The partially reduced enzyme is then mixed in a stopped-flow apparatus with more concentrated buffer at another pH, and the redistribution of reducing equivalents among the several redox-active centers followed spectrophotometrically as the system achieves its new equilibrium position. This methodology is particularly well suited to systems having a combination of centers with strongly pH-dependent reduction potentials (*e.g.* flavins) and others that are less pH-dependent (*e.g.* iron-sulfur centers and hemes). In such cases, the pH jump is expected to perturb the equilibrium distribution of reducing equivalents within the enzyme. It is a particular advantage of the method that it specifically selects for those electron transfer processes that are coupled to protonation/deprotonation events, since those that are not do not respond to the pH jump.

Pulse radiolysis, like flash photolysis, involves rapidly introducing reducing equivalents and following subsequent intramolecular equilibration spectrophotometrically. Pulse radiolysis is very useful in that, apart from the superior time resolution over methods relying on rapid mixing of solutions, the concentration of the one-electron reduced enzyme species can be quantified accurately on the basis of the number of reducing equivalents generated in the radiolytic pulse (as determined by calibration against a chemical standard using dosimetry).

The specific systems we have examined previously are xanthine oxidase (3–6) and trimethylamine dehydrogenase (7–9), two flavin-containing enzymes containing multiple redox-active centers. Xanthine oxidase possesses a molybdenum center, two 2Fe/2S centers of the spinach ferredoxin variety and flavin adenine nucleotide (10). The distribution of reducing equivalents among these centers has been shown to depend strictly on their relative reduction potentials (11), which are known to be pH-dependent (12). The specific electron equilibration process within partially reduced enzyme that can be followed using the pH jump protocol is between the FAD and the iron-sulfur center designated Fe/S I (3, 5). The process is depicted in Scheme 1.

Electron transfer and deprotonation of the flavin semiquinone are tightly coupled in the above process, with deprotonation of the neutral flavin semiquinone occurring concomitantly with electron transfer from the semiquinone to the iron-sulfur



* This work was supported by National Institutes of Health Grants GM58481 and GM59953 (to R. H.) and by travel support through National Science Foundation Grant INT 9513747. The costs of publication of this article were defrayed in part by the payment of page charges. This article must therefore be hereby marked "*advertisement*" in accordance with 18 U.S.C. Section 1734 solely to indicate this fact.

§ To whom correspondence should be addressed: Dept. of Molecular and Cellular Biochemistry, Ohio State University, 333 Hamilton Hall, 1645 Neil Ave., Columbus, OH 43210-1218.

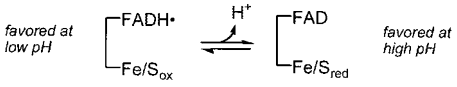


SCHEME 1

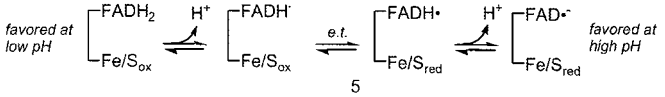


SCHEME 2

center (5). In other words, the flavin $N_5$-H bond of the neutral semiquinone is being cleaved and the proton is in motion as the system traverses (or tunnels through) the transition state for electron transfer. This conclusion is based on the observation of well behaved single-exponential kinetics for electron transfer in both the forward and reverse directions, in conjunction with the observation of large solvent kinetic isotope effects (between 7 and 10), and linear proton inventories (5). The observed rate constant for the reaction also exhibits only a modest, linear pH dependence, approximately doubling from 155 $s^{-1}$ at pH 6 to 330 $s^{-1}$ at pH 10.

In addition to the oxidation-reduction equilibration involving Fe/S I and FAD, which can be followed experimentally by stopped flow, a comparison of the static and kinetic spectral changes seen in the pH jump experiments indicates that a second process, involving Fe/S I and the molybdenum center, takes place in the dead time of the stopped-flow experiment (3). This faster process cannot be explicitly examined using the pH jump protocol but has been investigated by pulse radiolysis (4, 6). Using the radiolytically generated radical of *N*-methylnicotinamide ($NMN^{\cdot}$)[1] to rapidly and selectively reduce the molybdenum center of the enzyme, we have determined a rate constant for subsequent redox equilibration between the molybdenum and Fe/S I center of 8,600 $s^{-1}$ at pH 8.5 (6). The observed rate constant is in good agreement with that expected on the basis of Marcus theory for electron transfer, given the distance between donor and acceptor (13, 14) and assuming a value for the rate decay parameter $\beta$ in the range normally seen in proteins (~1.4 $Å^{-1}$).

Trimethylamine dehydrogenase is a simpler system than xanthine oxidase, possessing a single 4Fe/4S (bacterial ferredoxin-type) cluster and a covalently linked 6-cysteinyl FMN. Electron transfer between the iron-sulfur center and flavin within two-electron reduced enzyme has been studied previously using the pH jump technique (7, 8). The process is found to exhibit a large solvent kinetic isotope effect of 7–8 (8), although in this case the kinetic behavior of the system is more complicated than is seen with xanthine oxidase. Particularly in $D_2O$, the observed kinetics deviate significantly from single-exponential behavior, with lag phases seen in the high-to-low pH jump experiments and biphasic kinetics seen in the reverse direction. The observed rate constant in $H_2O$ also exhibits an unusual inverse bell-shaped pH dependence, with rate constants in the range of 300 to greater than 1,000 $s^{-1}$. The data obtained with trimethylamine dehydrogenase are best accounted for by assuming discrete steps for protonation and electron transfer, rather than the concomitant process seen with xanthine oxidase (Scheme 2).

In this scheme, electron transfer is assumed to be fast (in excess of 1,000 $s^{-1}$), with the observed kinetics rate-limited by the protonation/deprotonation events associated with electron transfer. Using established p$K_a$ values of 8.0 and 6.0 for the flavin semiquinone and hydroquinone, respectively, and assuming diffusion-controlled protonation steps, Scheme 2 is able to account not only for the observed kinetic behavior of electron transfer but also, significantly, for the pH dependence of the observed rate constant for electron transfer within two-electron reduced enzyme (7).

It is important to note that, in trimethylamine dehydrogenase, the flavin couple involved in the oxidation-reduction equilibrium is the semiquinone/hydroquinone couple rather than the quinone/semiquinone couple observed with xanthine oxidase. Nevertheless, the principal basis for the different behavior exhibited by xanthine oxidase and trimethylamine dehydrogenase apparently has to do with the extent to which the protein environment of the flavin center preferentially stabilizes the neutral *versus* the anionic form of the flavin in its reduced state (8). In the case of xanthine oxidase, this is the flavin semiquinone, and the protein is known to preferentially stabilize the neutral $FADH^{\cdot}$ form, as manifested in the typical long wavelength UV-visible absorbance and relatively broad EPR linewidths exhibited by the flavin semiquinone (15). By destabilizing the anionic form of the semiquinone, the protein prevents deprotonation of the $FADH^{\cdot}$ (acting as the electron donor) prior to electron transfer. At the same time, electron transfer is unlikely to precede deprotonation as formation of oxidized $FADH^+$ is extremely unfavorable thermodynamically. It is this combination of factors that dictates that flavin deprotonation be concomitant with electron transfer to other sites in the enzyme. By contrast to xanthine oxidase, trimethylamine dehydrogenase does not preferentially stabilize the neutral or anionic form of either the flavin hydroquinone or semiquinone oxidation state (8). The p$K_a$ values for both the semiquinone and hydroquinone are comparable to their values (Refs. 8 and 6, respectively) for the free cofactor (7). As a result, the protein environment of the flavin does not prevent deprotonation prior to electron transfer, as is the case with xanthine oxidase, and deprotonation and electron transfer are thus able to proceed via discrete chemical steps rather than concomitantly.

Other redox-active centers in addition to flavins are known to take up protons upon reduction, and particularly in the case of molybdenum centers, such as that found in xanthine oxidase, it has been clearly demonstrated that reduction of Mo(VI) to Mo(IV) is associated with proton uptake by ligands in the metal coordination sphere (16, 17). This redox-linked protonation can be formulated as follows (Scheme 3).

This scheme is consistent with x-ray spectroscopic studies of the fully oxidized and reduced forms of the enzyme, in which protonation of the Mo=S group upon reduction of the center is manifested as a significant lengthening of the Mo–S bond (18–20). Comparable changes are seen crystallographically upon reduction of the aldehyde oxidoreductase from *Desulfovibrio gigas* (21), another member of the molybdenum hydroxylase family of enzymes. Furthermore, EPR studies of the Mo(V) oxidation state have demonstrated the presence of two inequivalent protons in the predominant EPR-active Mo(V) species formed at pH 8.5 (22); these have been assigned to be the Mo-SH and Mo-OH protons of the center species of Scheme 3 (Ref. 10, and references therein). Although formation of the oxidized Mo(VI)SH species shown in *parentheses* in Scheme 3 cannot be rigorously excluded, x-ray spectroscopic studies have demonstrated that the Mo=S bond of oxidized enzyme does not protonate at as low a pH as 6.0 (as evidenced by no lengthening of the Mo-S bond).[2] It thus appears unlikely that a protonated Mo(VI)-SH species is an intermediate in the first reductive step of the scheme. Similarly, density functional calculations have

[1] The abbreviations used are: $NMN^{\cdot}$, the one-electron reduced radical of *N*-methylnicotinamide; $NMN^+$, *N*-methylnicotinamide.

[2] R. Hille, G. N. George, and S. P. Cramer, unpublished data.

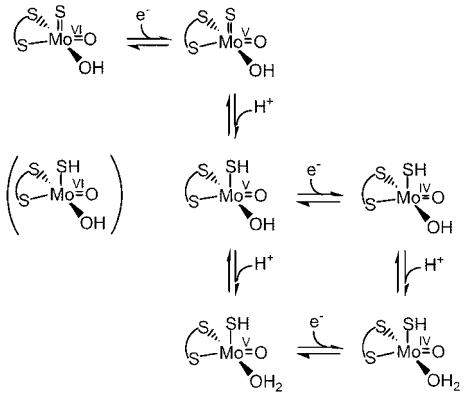

SCHEME 3

shown that, once the molybdenum becomes reduced to the Mo(IV) state, the Mo-OH group of oxidized enzyme exists predominantly as Mo-$OH_2$ (23).

The overall uptake of protons upon reduction of the molybdenum as indicated in Scheme 3 is an intrinsic property of the center, just as is the case with the flavin, raising the question as to whether this occurs concomitantly with reduction or oxidation of the center, or as a discrete chemical step. In order to further examine electron transfer within xanthine oxidase and trimethylamine dehydrogenase, specifically with regard to the role of protonation/deprotonation events associated with electron transfer, we have undertaken the present solvent kinetic isotope effect study of electron transfer within these enzymes using pulse radiolysis.

## MATERIALS AND METHODS

Xanthine oxidase was purified from cow's milk obtained from the experimental dairy herd at the Ohio State University using a variation on the protocol of Massey *et al.* (24), as described previously (25). Enzyme concentration was determined from the absorbance at 450 nm using an extinction of 37.8 $mM^{-1}$ $cm^{-1}$ (24). Trimethylamine dehydrogenase was purified from *Methylophilus methylotrophus* $W_3A_1$ as described by Steenkamp and Mallinson (26), except that gel filtration was performed using Sephacryl S-200 rather than Sephadex G-200. An extinction coefficient of 27.3 $mM^{-1}$ $cm^{-1}$ at 442 nm was used to determine the enzyme concentration (27).

*N*-Methylnicotinamide was purchased from Sigma, and $D_2O$ from Cambridge Isotopes Laboratory. All other buffers and reagents were of the highest purity commercially available and were used without further purification. Buffered solutions in $D_2O$ were prepared using carefully dried reagents, adjusting the pH meter reading by 0.4 to correct for the effect of $D_2O$ (28).

Pulse radiolysis was performed using the 4-MeV Dynaray linear accelerator facility at the University of Auckland (Auckland, New Zealand), which possesses a computer-controlled custom-built detection system fitted with Supracil optics. 200-ns electron pulses of sufficient power to give radiolytic doses on the order of 4–6 Gy (J/kg) were used to initiate reactions under controlled conditions, with dosimetry being carried out before each experimental run to quantify the yield of radicals generated with each pulse. Potassium thiocyanate (at a concentration of 10 mM) was the dosimetry standard, using a radiation chemical yield for $(SCN)_2^-$ of 0.29 $\mu$mol/J and an extinction coefficient of 7.58 $mM^{-1}$ $cm^{-1}$ for the radical at 475 nm (29). Under the experimental conditions used in the present study, the initially generated radiolytic radicals are $e_{aq}^-$, $HO^\bullet$ and $H^\bullet$, which in $N_2O$-equilibrated buffer solutions containing 0.1 M sodium formate are converted to $CO_2^-$ within the duration of the 200-ns electron pulse. $CO_2^-$ in turn quantitatively reduces *N*-methylnicotinamide (present at a concentration of 2.5 mM in the present experiments), generating $NMN^\bullet$ within 1 $\mu$s of the electron pulse. Under the experimental conditions used here, 0.68 $\mu$M $NMN^\bullet$ was generated per Gy of radiolytic pulse (30). It is the strongly reducing $NMN^\bullet$ (the reduction potential for the $NMN^+/NMN^\bullet$ couple is $-1.01 \pm 0.2$ V; Ref. 31) that represents the proximal reductant of enzyme in the present protocol; $NMN^\bullet$ has been shown to react with xanthine oxidase and trimethylamine dehydrogenase with second-order rate constants in excess of $10^8$ $M^{-1}$ $s^{-1}$ (6, 9). Thus, under our experimental conditions of ~100 $\mu$M enzyme, xanthine oxidase and trimethylamine dehydrogenase are reduced by $NMN^\bullet$ with pseudo first-order rate constants considerably in excess of $10^4$ $s^{-1}$, making it possible to follow subsequent slower intramolecular electron transfer processes spectrophotometrically.

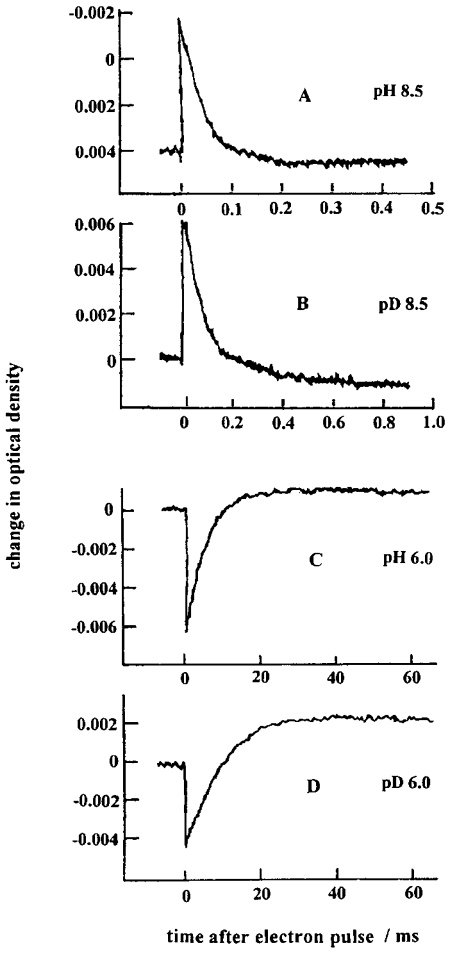


FIG. 1. **Kinetic transients observed in the course of the reaction of $NMN^\bullet_2$ with xanthine oxidase at different pH/pD and concentrations of the protein.** The first two kinetic phases followed for pH/D 8.5 are at 393 nm (*panels A* (75 $\mu$M) and *B* (89 $\mu$M)), the third kinetic phase followed for pH/D 6.0 is at 525 nm (*panels C* (64 $\mu$M) and *D* (70 $\mu$M)).

## RESULTS

*Solvent Kinetic Isotope Effects on Electron Transfer within Xanthine Oxidase*—We have previously shown that the initial reduction of xanthine oxidase by $NMN^\bullet$ occurs at the molybdenum center, with the absorbance change associated with the reaction due to oxidation of the radiolytically generated $NMN^\bullet$ (6). The overall reaction of xanthine oxidase with $NMN^\bullet$ at pH 8.5 is biphasic: a fast phase involving an absorbance decrease at 393 nm due to reduction of the molybdenum center by the $NMN^\bullet$, and a slower phase involving a subsequent absorbance decrease in the 390–550-nm region due to subsequent electron transfer from the molybdenum to the iron-sulfur centers. These results are accurately reproduced in the present work (Fig. 1; fitted lines have been omitted for clarity, typical uncertainties were in the range of 15–25%, see Tables I and II). Analysis of the initial phase of the reaction, which reflects reaction of the enzyme with $NMN^\bullet$, indicates that the enzyme is reduced with a second-order rate constant, $k_1$, in the range 3.3 to 7.4 $\times$ $10^8$ $M^{-1}$ $s^{-1}$ under the present conditions (21 °C and 75 $\mu$M enzyme, calculated from an observed rate constant of 25,000 $s^{-1}$), somewhat slower than seen in previous work ($9 \times 10^8$ $M^{-1}$ $s^{-1}$; Ref. 6), but generally consistent. When the reaction was repeated in

TABLE I

*Rate constants of electron transfer in xanthine oxidase*

Table shows data from pulse radiolysis (~10 Gy in 200 ns) of xanthine oxidase ([XO]), sodium formate (0.1 M), *N*-methylnicotinamide (2.5 mM) in $N_2$)-saturated phosphate (10 mM) buffered $H_2O$ (pH) and $D_2O$ (pD) solutions.

| pH/pD | [XO] | $10^{-4}\ k_1$ | $10^{-3}\ k_2$ | $k_3$ |
|---|---|---|---|---|
| | $\mu M$ | $s^{-1}$ | $s^{-1}$ | $s^{-1}$ |
| pH 6.0 | 64* | 3.7 ± 0.4 (1)[a] | 8.2 ± 0.8 (1)[a] | 190 ± 18 (4)[a] |
| | 95 | 7.0 ± 1.6 (2) | 12.3 ± 0.9 (2) | ND |
| | 117 | ND | ND | 171 ± 32 (4) |
| | 105 | 4.3 ± 1.6 (2) | 11.3 ± 1.7 (2) | 138 ± 14 (2) |
| | 30 | 3.6[b] | 8.5[b] | |
| | 50 | 4.1[b] | 8.5[b] | ND |
| | 70 | 6.4[b] | 8.6[b] | 125 |
| | 100 | 8.2[b] | 8.7[b] | ND |
| pD 6.0 | 70* | 5.0 ± 0.5 (2)[a] | 9.9 ± 1.0 (2)[a] | 101 ± 2 (2)[a] |
| | 175* | 8.7 ± 2.0 (2)[a] | 15 ± 5 (2)[a] | 96 ± 7 (3)[a] |
| | 93 | 6.3 ± 2.6 (3) | 13.1 ± 2.0 (3) | 51 ± 5 (3) |
| | 99 | 7.6 ± 1.1 (2) | 17 ± 4.0 (2) | 47 ± 2 (3) |
| pH 8.5 | 75 | 2.5 ± 0.3 (2) | 10.1 ± 0.4 (2) | NR |
| | 32 | 3.7[b] | 8.4[b] | NR |
| | 50 | 5.2[b] | 8.5[b] | NR |
| pD 8.5 | 89 | 2.0 ± 0.2 (3) | 4.5 ± 1.5 (3) | NR |

[a] Data at temperature 26 ± 0.2 °C, other data at 21 ± 1 °C; ND, not determined; NR, no reaction seen; number of transients analysed given in parentheses; wavelengths of observation for $k_1$ and $k_2$ (393, 420 nm) and $k_3$ (525 nm).

[b] Data are from Anderson and Hille (Ref. 6).

TABLE II

*Rate constants of electron transfer in trimethylamine dehydrogenase*

Data from pulse radiolysis (~10 Gy in 200 ns) of trimethylamine dehydrogenase ([TMADH]), sodium formate (0.1 M), *N*-methylnicotinamide (2.5 mM) in $N_2$-saturated phosphate (10 mM) buffered $H_2O$ (pH) and $D_2O$ (pD) solutions. Temperature 21 ± 2 °C; number of transients analysed given in parentheses; wavelengths of observation for $k_1$ (393, 475 nm) and $k_2$ (365, 475 nm).

| pH/pD | [TMADH] | $10^{-4}\ k_1$ | $k_2$ |
|---|---|---|---|
| | $\mu M$ | $s^{-1}$ | $s^{-1}$ |
| pH 6.0 | 126 | 3.39 ± 0.67 (3) | 1603 ± 403 (10) |
| | 143 | 3.1 ± 1.0 (2) | 1274 ± 184 (6) |
| pD 6.0 | 117 | 1.46 ± 0.11 (4) | 147 ± 40 (8) |
| pH 8.5 | 40 | 0.74 (1) | 159 ± 36 (4) |
| | 130 | 2.21 ± 0.20 (3) | 156 ± 28 (5) |
| pD 8.5 | 107 | 4.84 (1) | 116 ± 5 (2) |

$D_2O$, the observed rate constant was essentially the same (within experimental error) as that seen in $H_2O$, with a value of 20,000 $s^{-1}$ (at 90 $\mu$M enzyme). This indicated that the initial reduction of the enzyme molybdenum center was essentially independent of solvent isotope and therefore uncoupled from protonation, the implication being that reduction precedes protonation on generation of the initially formed Mo(V) species.

The second kinetic phase observed in the reaction at pH 8.5 exhibits a rate constant previously shown to be independent of protein concentration and wavelength dependence, including a further absorbance decrease at 393 nm, consistent with electron transfer from the molybdenum center to one of the Fe/S centers (6). The rate constant $k_2$ of ~10,100 $s^{-1}$ seen in the present work (Fig. 1*A*; Table I) is in reasonable agreement with these previous results (8,600 $s^{-1}$; Ref. 6). When the experiment was repeated in $D_2O$ (Fig. 1*B*), the observed rate constant for this slower phase was reduced by a factor of approximately 2, to 4,500 $s^{-1}$ (Fig. 1; Table I). Thus, in contrast to the initial reduction of the molybdenum center, its subsequent reoxidation by electron transfer to the iron-sulfur centers of the enzyme was at least partially coupled to its deprotonation. It is to be emphasized that, for a solvent kinetic isotope effect to be manifested on this phase of the reaction, the molybdenum center must have become protonated (at a diffusion-controlled rate) subsequent to its initial reduction to the Mo(V) state in the fast phase of the reaction.

At pH 8.5, the relative reduction potentials of the four redox-active centers of xanthine oxidase are such that the equilibrium distribution of the radiolytically introduced reducing equivalent within one-electron reduced enzyme favors iron-sulfur reduction (11, 12), and no spectral change subsequent to that seen for the molybdenum-to-Fe/S electron transfer is expected or observed. On lowering the pH to 6, however, a significant amount of flavin semiquinone is expected (5, 12), and indeed on a longer time scale than that seen at pH 8.5, an additional kinetic phase is observed (6). The wavelength dependence of this kinetic phase is consistent with electron transfer from the iron-sulfur centers of the enzyme to the flavin to give the semiquinone, including a significant absorbance increase at 525 nm. The rate constant seen in the present work (166 $s^{-1}$ averaged from three separate experiments; Fig. 1*C* and Table I) was in good agreement with that seen in previous pH jump studies (155 $s^{-1}$; Ref. 3). and pulse radiolysis work (125 $s^{-1}$; Ref. 6). In $D_2O$, the observed rate constant was reduced to 74 $s^{-1}$ (average of Fig. 1*D*, Table I). The magnitude of the solvent kinetic isotope effect, 2.2, was approximately one third that seen in previous pH jump studies (6.9), a result that presumably has to do with ionizations in addition to those associated with the flavin center being involved in the pH jump experiments, but not in the radiolytic experiment.

*Solvent Kinetic Isotope Effect on Electron Transfer within Trimethylamine Dehydrogenase*—As with xanthine oxidase, the reaction of $NMN^{\cdot}$ with trimethylamine dehydrogenase is multiphasic. Previous work has shown that the initial phase of the reaction is again dependent on the concentration of protein, with an approximately pH-independent second-order rate constant of $2 \pm 0.2 \times 10^8$ $M^{-1}$ $s^{-1}$ (9). At pH 8.5, the spectral change associated with the initial phase of the reaction indicates that the principal site of reaction with $NMN^{\cdot}$ is the 4Fe/4S center of the enzyme (9). (Although the Fe/S center lies rather deeply buried in trimethylamine (~10 Å from the protein surface at closest approach; Ref. 32), previous work has demonstrated the existence of a redox-active "hot spot" in the vicinity of Tyr-442 that is involved in electron transfer from the Fe/S center to the physiological electron acceptor for trimethylamine dehydrogenase, an electron-transferring flavoprotein; Ref. 33.) In the present work, the observed rate constant for this fast phase of the reaction is $1.8 \times 10^8$ $M^{-1}$ $s^{-1}$ (average of two experiments: $k_{obs}$ = 7,400 $s^{-1}$ with 40 $\mu$M enzyme and 22,100 $s^{-1}$ with 130 $\mu$M enzyme; Table II), consistent with this earlier work. It is significant that, under the present experi-

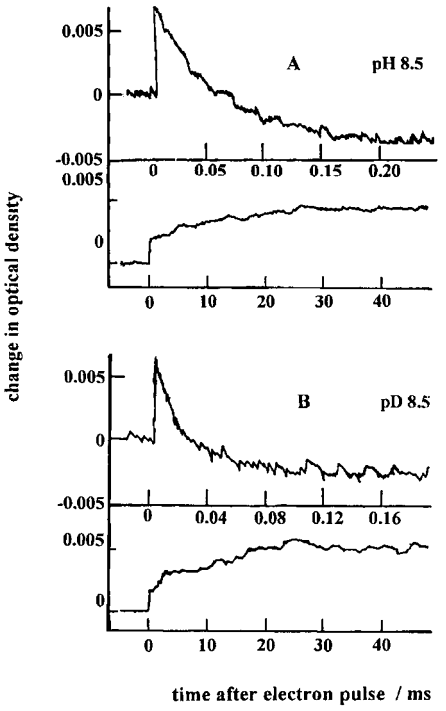


FIG. 2. **Kinetic transients observed in the course of the reaction of NMN˙ with trimethylamine dehydrogenase at pH/pD 8.5.** *Panel A*, pH 8.5, 130 $\mu$M; *panel B*, pD 8.5, 107 $\mu$M. In both panels the *upper traces* are at 396 nm and the *lower traces* at 365 nm, following decay of the NMN˙ radical and formation of the anionic flavin semiquinone, respectively.

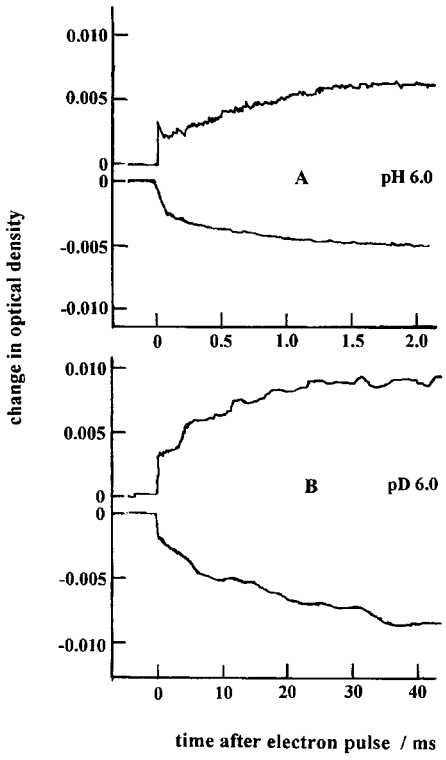


FIG. 3. **Kinetic transients observed in the course of the reaction of NMN˙ with trimethylamine dehydrogenase at pH/pD 6.0.** *Panel A*, pH 6.0, 143 $\mu$M; *panel B*, pD 6.0, 117 $\mu$M. In both panels the *upper traces* are at 365 nm and the *lower traces* at 475 nm, following formation of the flavin semiquinone and oxidation of the iron-sulfur center, respectively.

mental conditions, NMN˙ reduces the enzyme sufficiently rapidly even in $D_2O$ (with a pseudo first-order rate constant of 48,000 $s^{-1}$; Fig. 2*B* and Table II) for internal electron transfer taking place subsequent to the initial reduction event to be followed kinetically.

A slower kinetic phase was observed subsequent to the initial reduction event whose rate was independent of protein concentration; the associated spectral change, exhibiting an absorbance decrease at 396 nm and an increase at 365 nm (Fig. 2*A*), is consistent with a small amount of electron transfer from the initially reduced Fe/S center to the enzyme flavin to give the flavin anionic semiquinone. The observed rate is 158 $s^{-1}$ (Table II), again consistent with previous work (9). On going to $D_2O$, the observed rate constant for this slower phase decreased to 116 $s^{-1}$ in $D_2O$ (Fig. 2*B*; Table II), indicating that the observed process was only very modestly dependent on solvent isotope. This result is expected, given that the p$K_a$ of the flavin semiquinone is ~8 and it is thus principally the anionic form that is generated at pH 8.5. With little protonation of the flavin upon reduction, only a small solvent kinetic isotope effect is expected. The observed rate constant in $H_2O$ determined here is slower than is seen using the pH jump protocol (~400 $s^{-1}$; Refs. 3 and 5). Although the present experiments were carried at a somewhat lower temperature (21 °C rather than 25 °C in the case of the pH jump experiments), we attribute this difference primarily to the fact that the pH jump experiment followed electron transfer in two-electron reduced enzyme (involving electron transfer from the reduced Fe/S center to the flavin semiquinone to give the hydroquinone), whereas in the present case electron transfer is within one-electron reduced enzyme (involving electron transfer from the reduced Fe/S center to oxidized flavin to give the flavin semiquinone).

At pH 6.0, the fast kinetic phase of the initial reaction of NMN˙ with trimethylamine dehydrogenase exhibited kinetics with an observed rate constant of 33,900 $s^{-1}$ with 126 $\mu$M enzyme and 31,000 $s^{-1}$ at 143 $\mu$M (Table II), yielding a second-order rate constant for reaction of enzyme with NMN˙ of $2.42 \times 10^8$ $M^{-1}$ $s^{-1}$ (average of two experiments) consistent with previous work indicating a value of $2.0 \pm 0.2 \times 10^8$ $M^{-1}$ $s^{-1}$ (9). The slower phase of the reaction exhibited an increase at 365 nm and a decrease at 475 nm (Fig. 3*A*), again indicative of electron transfer from the 4Fe/4S center to the enzyme flavin. (On the basis of the observed spectral change, it was principally the anionic semiquinone that accumulates, although some blue neutral semiquinone is expected.) The observed rate constant for this process was 1,603 ± 403 $s^{-1}$ (126 $\mu$M enzyme) and 1,274 ± 184 $s^{-1}$ (143 $\mu$M enzyme); although there is some uncertainty, the lower rate constant is observed at the higher protein concentration, and we conclude that the observed kinetics are independent of protein concentration with a value of ~1,440 $s^{-1}$, in fairly good agreement with the previously determined value of 1,860 ± 260 $s^{-1}$ (9). The observed rate constant is, however, severalfold faster than that seen under comparable conditions using the pH jump protocol (440 $s^{-1}$; Refs. 3 and 5). Again, the difference in observed rate constant in the pulse radiolysis and pH jump protocols is attributed to the different level of enzyme reduction in the two experiments.

In $D_2O$, the observed rate constant for the internal electron transfer step decreased from ~1,500 $s^{-1}$ to 147 ± 40 $s^{-1}$(Fig. 2, Table II), reflecting a solvent kinetic isotope effect of ~10 Although the uncertainty in the determination is large (±4), the results are generally consistent with previous work, in which a value of 13.4 ± 1.9 was reported (9). The magnitude of the present error notwithstanding, it is clear that the solvent kinetic isotope effect on electron transfer to oxidized flavin seen here in one-electron reduced enzyme is large (>6) and comparable to that seen on electron transfer to the flavin semiquinone in two-electron reduced enzyme (to generate the flavin

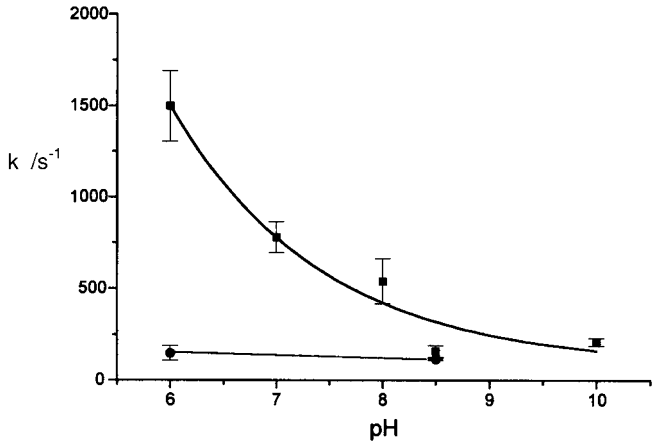


FIG. 4. **The pH dependence of the observed rate constant for electron transfer equilibration from the 4Fe/4S center to the 6-cysteinyl-FMN center of trimethylamine dehydrogenase.** *Solid squares*, data in $H_2O$, *solid circles*, in $D_2O$. Conditions are as described in the text. The nonlinearity of the plot in $H_2O$, distinguishing it from comparable data for xanthine oxidase (3), is readily evident.

hydroquinone) in the previous pH jump experiments (with a solvent kinetic isotope effect of ~8; Ref. 8).

The overall pH dependence of the observed rate constant for electron transfer from the 4Fe/4S center of trimethylamine dehydrogenase to its 6-cysteinyl-FMN as determined by pulse radiolysis is shown in Fig. 4, where it can be seen that it is distinctly non-linear. The observed rate constants are dependent on the $\Delta E$ between the two redox-active centers and will depend individually on the different protonation and ionization states of the participating centers. At high pH neither center presumably has an ionizable proton (for the flavin it is the anionic semiquinone which predominates at this pH), and the observed rate constant is independent of pH. At lower pH some protonation of the flavosemiquinone is expected upon reduction, and the observed increase in the rate of electron equilibration most likely reflects an increase in the one-electron reduction potential of this center relative to that for the Fe/S center. The result is reminiscent of the pH dependence seen for electron transfer in the two-electron reduced enzyme (8), and as in this earlier work we conclude that, although the observed solvent kinetic effect is large, the system is best described as having discrete ionization and electron transfer steps in the course of the overall reaction.

## DISCUSSION

*Electron Transfer in Xanthine Oxidase*—Our results in the present work not only confirm previous results (3, 5), but extend a solvent kinetic isotope analysis to electron transfer between the molybdenum and iron-sulfur centers of the enzyme. At pH 8.5, initial reduction of the molybdenum center does not, within experimental error, exhibit a solvent kinetic isotope effect. On the other hand, the subsequent electron equilibration with the iron-sulfur center does, with $k_{obs}$ decreasing from 10,100 $s^{-1}$ to 4,500 $s^{-1}$ on going from $H_2O$ to $D_2O$. The modest solvent kinetic isotope effect thus observed, ~2.2, must arise from the fact that the molybdenum center, once reduced by NMN$^{\cdot}$, protonates prior to electron transfer on to the iron-sulfur centers. EPR studies have shown that protonation of the Mo=S moiety at the Mo(V) oxidation state occurs at pH 8.5 (22), and this process is reasonably expected to be diffusion-controlled. The molybdenum center must eventually deprotonate upon reoxidation to Mo(VI) upon electron transfer to the Fe/S center(s), as the oxidized center is known to possess an unprotonated Mo=S group even at pH 6.0. It is thus most likely that the Mo-SH proton is responsible for the observed solvent kinetic isotope effect on electron transfer.[3]

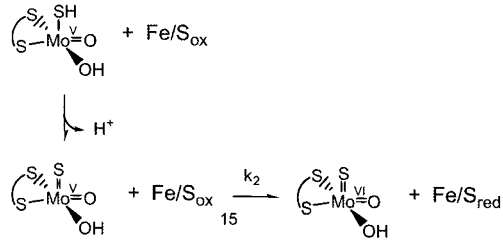


SCHEME 4

The solvent kinetic isotope effect seen for electron transfer from the molybdenum to the iron-sulfur centers is not particularly large. Two likely explanations exist: either the reaction proceeds via an "early" transition state (in which case the isotope effect would not be expected to be fully expressed), or deprotonation of the molybdenum center is not strictly coupled to electron transfer. In this latter case, the overall process involves separate chemical equilibria, and electron transfer from the molybdenum center to Fe/S I can be summarized as shown in Scheme 4.

If the forward process (*i.e.* in the direction of physiological electron transfer, from the molybdenum center to Fe/S I) involves discrete steps for protonation/deprotonation and electron transfer, then a Marcus treatment of the data is not appropriate, as the observed rate constant does not reflect the intrinsic rate of electron transfer in the system. If, on the other hand, the process involves a single step (with an early transition state to account for the small value of the solvent kinetic isotope effect determined here), it is possible to analyze the data in the context of Marcus theory for electron transfer (34, 35). The x-ray crystal structures of the aldehyde oxidoreductase from *D. gigas*, the CO dehydrogenase from *Oligotropha decarboxidovorans*, as well as that of bovine xanthine oxidase, have been reported (13–15), and in each the molybdenum center is found to be 14.5 Å from the nearer of the two iron-sulfur centers, with the pyranopterin of the molybdenum center (represented in Schemes 2 and 4 as the two thiolate sulfurs to the left of the metal) intervening (Fig. 5). The distal amino group of the cofactor is in fact hydrogen-bonded to a cysteine ligand of the proximal iron-sulfur center, a structural element that is highly conserved in these enzymes. It has been known for some time that the two iron-sulfur centers of xanthine oxidase, while exhibiting nearly identical UV-visible and circular dichroism properties (37), give rise to distinct EPR signals (38). It has also been shown that Fe/S I magnetically couples to the molybdenum center under certain conditions (39, 40), suggesting that Fe/S I is the proximal iron-sulfur cluster in the crystal structure. The assignment of Fe/S I as the proximal iron-sulfur cluster to the molybdenum center has recently been confirmed for CO dehydrogenase (41), aldehyde oxidoreductase (42), and xanthine oxidase (43).

With the assignment of the iron-sulfur clusters established, it is possible to examine electron transfer from the molybdenum to Fe/S I in greater detail in light of the newly available structural information. The reduction potentials for the

[3] The so-called "rapid type 1" EPR signal that predominates under the present experimental conditions exhibits coupling to two inequivalent protons, one more strongly coupled at 12 gauss and the other more weakly coupled at 4 gauss (22). The former has been assigned to the Mo-SH group and the latter to the Mo-OH (see Ref. 10, and references therein). That the former center deprotonates upon reoxidation to the Mo(VI) valence state while the latter remains as Mo-OH justifies the assignment of the former as the site responsible for the observed solvent kinetic isotope effect.

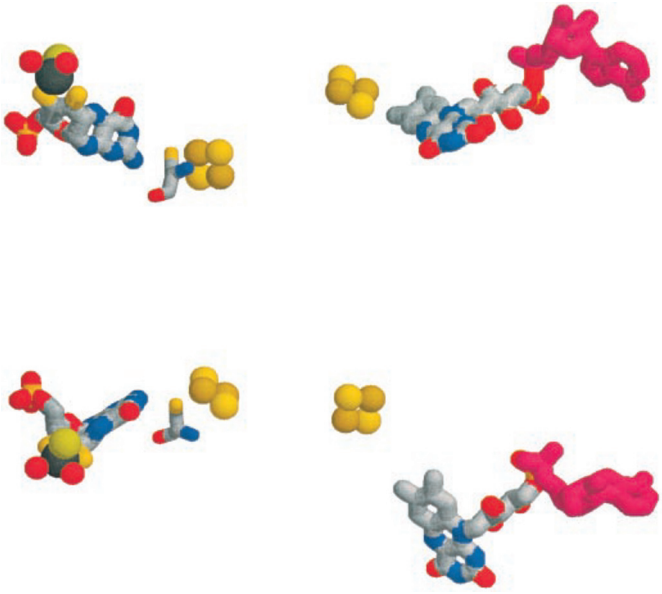

FIG. 5. **Disposition of the redox-active centers in xanthine oxidase.** The molybdenum atom is rendered in *gray* on the *left*, the flavin in CPK on the *right*, with the two iron-sulfur centers Fe/S I (nearer the molybdenum center) and Fe/S II (nearer the flavin) intervening. The *lower representation* has been rotated 90° about the horizontal with respect to the *upper representation*. The cysteine residue ($Cys^{150}$) to which the distal amino group of the pyranopterin cofactor of the molybdenum center is hydrogen-bonded is also shown (most clearly evident in the *lower representation*). Figure is modeled after Enroth *et al*. (13).

Mo(VI)/Mo(V) and Fe/S I couples at pH 8.5 are −375 mV and −335 mV, respectively (12), yielding a driving force of 0.9 kcal/mol and an equilibrium constant of 4.6 (in favor of Fe/S I reduction).[4] The observed kinetics involves the approach to an oxidation-reduction equilibrium between the two centers, and as such represents the sum of the forward and reverse electron transfer rate constants. The equilibrium constant represents the ratio of these two rate constants, permitting the forward and reverse rates of electron transfer to be calculated explicitly. With values of 10,100 $s^{-1}$ for the approach to equilibrium (present work) and 4.6 for the effective equilibrium constant at pH 8.5 (from the reduction potentials above), rate constants for Mo-to-Fe/S I electron transfer and the reverse are calculated to be 8,300 and 1,800 $s^{-1}$, respectively. Using a distance, $r_{DA}$, of 14.5 Å (13–15) between the two centers and the expression for electron transfer used in Marcus theory, $k = A\exp[-\beta r_{DA}]$, it is possible to calculate the exponential decay rate with distance ($\beta$). Assuming a pre-exponential factor of $10^{13}$ $s^{-1}$, $\beta = 1.4$ $Å^{-1}$ for electron transfer from the molybdenum center to Fe/S I. This is in good agreement with the value that is commonly found for electron transfer in proteins (44, 45), indicating that the pyranopterin cofactor confers no particularly effective electron transfer pathway between the molybdenum center and Fe/S I. Indeed, recent magnetic circular dichroism studies of xanthine oxidase have led to the proposal that electron transfer out of the molybdenum center is mediated by $\sigma$ rather than $\pi$ interactions with the redox-active $d_{xy}$ orbital of the molybdenum center (46). The upshot is that the limited $\pi$-conjugation of the pyranopterin cofactor of the molybdenum center (which is present in the protein as a ring-closed pyran that is equivalent to a tetrahydro form devoid of $\pi$ electrons) is not sufficient to impart any particularly facile pathway for electron transfer out of the molybdenum center.

A similar analysis is also possible for electron transfer from Fe/S II to the flavin of xanthine oxidase. Given the spectroscopically silent nature of electron transfer between the two iron-sulfur centers, the physical disposition of the redox-active centers in the protein dictate that the spectrophotometrically observed process involves electron transfer between Fe/S II and the flavin, which are separated by an edge-to-edge distance of ~8.7 Å (13). Here it is important to recognize a distinction between the situation encountered in the present pulse radiolysis results and that found in the previous pH jump work (3, 5). The pH jump experiment necessarily follows the equilibration of a reducing equivalent between Fe/S I and the flavin, mediated, on the basis of the crystal structure, by Fe/S II despite the fact that the net level of reduction of Fe/S II does not change significantly in the course of the pH jump experiment. By contrast, in the present pulse radiolysis experiment, Fe/S II is initially oxidized, accepts an electron from Fe/S I then passes that electron on to the FAD; the spectrophotometrically observed process thus involves electron transfer from Fe/S II rather than Fe/S I in the pulse experiment. The good agreement of the observed rate constants for electron transfer seen in the present pulse radiolysis work and previous pH jump experiments suggests that electron transfer between the two iron-sulfur centers is not rate-limiting in the latter case. This implies that electron transfer between the two iron-sulfur centers is very fast, possibly on a time scale comparable to electron transfer between the molybdenum center and Fe/S I. Bearing this in mind, the relevant reduction potentials for consideration are those for Fe/S II and the flavin quinone/semiquinone couples, which have values at pH 6.0 of −155 and −200 mV, respectively, at pH 6.0 (12). These potentials yield an equilibrium constant of 5.6 (in favor of Fe/S II reduction) and with an observed rate constant of 170 $s^{-1}$ for the approach to equilibrium (present work; Refs. 5 and 6), the calculated rate constants for electron transfer from the iron-sulfur center to the flavin (generating the semiquinone) and the reverse are 25 $s^{-1}$ and 145 $s^{-1}$, respectively. These rate constants are very small, given the distance of 8.7 Å between donor and acceptor, a reflection of the fact that protonation/deprotonation is tightly linked to electron transfer between Fe/S and FAD in xanthine oxidase (5); in the Marcus formalism for electron transfer, this is due to a significant increase in the reorganizational energy for the electron transfer reaction.

That the redox-active centers of xanthine oxidase are not laid out in order of their reduction potentials deserves comment. Electron transfer from the molybdenum center to Fe/S I is reasonable as the two sites are nearly isopotential. The high potential Fe/S II, however, intervenes between Fe/S I and the flavin. This situation is not an uncommon one in biological systems, and as has been pointed out by Dutton and co-workers (44, 45), need not necessarily constitute a significant kinetic barrier to catalysis. It is important to recognize, however, how this arrangement influences the equilibrium distribution of reducing equivalents within the system, assuming (as is known to be the case for xanthine oxidase; Refs. 11, 47, and 48) that electron transfer among the centers is rapid compared with catalytic turnover. This "rapid equilibrium" situation leads to paradoxical behavior of xanthine oxidase in the course of reductive titrations. Thus, in one-electron reduced enzyme, the electron distribution within the enzyme is such that Fe/S II is ~62% reduced and Fe/S I 25% (the flavin semiquinone and Mo(V) states are each less than 10%; Ref. 11). By contrast, in

[4] At pH 8.5 electron transfer is expected to proceed on to Fe/S II (which has a considerably higher reduction potential than that of Fe/S I; −230 mV at pH 8.5; Ref. 12), but as the two iron-sulfur centers exhibit the same spectral changes on reduction, electron transfer from Fe/S 1 to Fe/S II is spectroscopically silent. The observed spectral change being followed in the present study must therefore arise from electron transfer from the molybdenum center to Fe/S I.

two-electron reduced enzyme, Fe/S II is only 35% reduced, Fe/S I 28% reduced, and the flavin 60% fully reduced to the level of the hydroquinone. The unexpected result is that addition of a second reducing equivalent to the one-electron reduced enzyme leads to *oxidation* of the high potential Fe/S II to a significant degree. This is a consequence of the fact that, although the first half-potential for the flavin is substantially lower than those of the iron-sulfur centers at pH 8.5, the midpoint potential for the flavin is comparable to the *average* of the reduction potentials for the two iron-sulfur centers. Thus, in one-electron reduced enzyme, little flavin semiquinone (or Mo(V)) is formed and the single reducing equivalent resides predominantly on Fe/S II (and to a lesser extent Fe/S I). Upon addition of a second reducing equivalent, however, the flavin hydroquinone can now form, with the result that the flavin center competes effectively for a *pair* of reducing equivalents with the two iron-sulfur centers. The significant point is that the relative reduction potentials for the iron-sulfur centers, with one high and one low, relative to the flavin midpoint potential, are such that reducing equivalents are effectively delivered to the flavin *in pairs*, despite the fact that the iron-sulfur centers themselves are strictly one-electron carriers; to a good first approximation, Fe/S II retains a single reducing equivalent until a second is available to reduce the flavin fully to the hydroquinone. The identical situation is also encountered in other systems possessing multiple redox-active centers and catalyzing two-electron chemistry, including hydrogenase (49, 50) and fumarate reductase (51). In both cases, the arrangement may well serve to ensure that reducing equivalents tend to be delivered to the active site (a Ni/Fe center in the case of hydrogenase,[5] a flavin in the case of fumarate reductase) in pairs.

*Electron Transfer in Trimethylamine Dehydrogenase*—In the case of trimethylamine dehydrogenase, the present work following the solvent kinetic isotope effect on electron transfer in one-electron reduced enzyme complements that done previously examining electron transfer within the two-electron reduced enzyme using the pH jump technique (8). Our present pulse radiolysis results indicate that electron transfer to the oxidized 6-cysteinyl-FMN to give the semiquinone in one-electron reduced enzyme exhibits a solvent kinetic isotope effect ($10 \pm 4$) at low pH comparable to that seen for electron transfer to the semiquinone to give the fully reduced hydroquinone in two-electron reduced enzyme (a value of ~8, Ref. 5). The pH dependence of the observed rate of electron equilibration in the present pulse radiolysis study is also reminiscent of that seen in the pH jump experiments. We conclude that protonation/deprotonation is best described as taking place in a separate chemical step from electron transfer in one-electron as well as in two-electron reduced enzyme (as determined previously using the pH jump method; Refs. 7 and 8).

*Contrasts between Xanthine Oxidase and Trimethylamine Dehydrogenase*—Differences in the solvent kinetic isotope effect for Fe/S → flavin electron transfer seen in xanthine oxidase and trimethylamine dehydrogenase are most marked at pH/pD 6. In the case of xanthine oxidase, a solvent kinetic isotope effect of ~2–3 is seen, whereas with trimethylamine dehydrogenase it is ~10. Both the type of Fe/S center (2Fe/2S and 4Fe/4S) and flavin (FAD and 6-cysteinyl-FMN) are different in the two proteins, but it is most likely that the difference in the behavior of the two proteins is related to differences in the environment of the flavin. Clearly, one factor is the extent to which the protein can accommodate one or another ionization state of the semiquinone and hydroquinone, as discussed in the Introduction. In addition, however, the degree of solvent accessibility and the mechanism of protonation/deprotonation may be important. A study of the fast one-electron reduction of the solvent-exposed FMN in the flavodoxin from *Megasphaera elsdenii* has shown that protonation of the anionic flavin semiquinone to give the neutral form occurs with a pH-independent, first-order rate constant of $1.1–2.6 \times 10^5\ s^{-1}$ (52). As this fast process is also observed at higher pH (9.15), it cannot arise from simple protonation and is also unlikely to be due to protonation of the anionic flavin semiquinone by nearby amino acid residues. Instead, protonation is likely to occur via rapid solvolysis of $H_2O$. Indeed, solvolysis in the protonation of the semiquinone anion of free FMN occurs at $\sim 4 \times 10^5\ s^{-1}$,[6] comparable to the rate constant observed with flavodoxin. Although the recent crystal structure of xanthine oxidase indicates that the FAD site is relatively solvent-accessible (13), the 6-cysteinyl-FMN in trimethylamine dehydrogenase is considerably more buried, with hydrophobic amino acid residues in the immediate vicinity of the flavin ring in the substrate binding site. Thus, access of bulk solvent to the flavin is more restricted in trimethylamine dehydrogenase as compared with xanthine oxidase. The reduction potentials of both the deeply buried Fe/S center and the 6-cysteinyl-FMN of trimethylamine dehydrogenase are pH-dependent (36), as is the strong magnetic interaction between the two centers as detected by EPR in the two-electron reduced enzyme (8). The pH dependence of the reduction potential for the Fe/S center is likely to arise from changes in the electrostatic environment due to protonation of ionizable amino acid residues in its immediate vicinity (including $His^{29}$, $His^{44}$, $His^{443}$, $Tyr^{442}$, $Tyr^{539}$, and $Cys^{320}$, all of which are within 10 Å of the 4Fe/4S center). The large solvent kinetic isotope effect seen on electron transfer from the Fe/S center to the flavin in trimethylamine dehydrogenase may well arise from coupling of electron transfer with protonation of these neighboring residues, in addition to protonation of the flavin to give the neutral semiquinone.

[5] Hydrogenase also is able to operate in the opposite direction, oxidizing $H_2$ by two electrons (53). The same argument presented here applies to the opposite direction of electron transfer; reducing equivalents will tend to leave the active site nickel center in pairs rather than individually, with little *kinetic* accumulation of the Ni(II) state).

[6] R. F. Anderson, unpublished data.

REFERENCES


1. Cukier, R. I. (1996) *J. Phys. Chem.* **100,** 15428–15443
2. Cukier, R. I., and Nocera, D. G. (1998) *Annu. Rev. Phys. Chem.* **49,** 337–369
3. Hille, R., and Massey, V. (1986) *J. Biol. Chem.* **261,** 1241–1247
4. Anderson, R. F., Hille, R., and Massey, V. (1986) *J. Biol. Chem.* **261,** 15870–15876
5. Hille, R. (1991) *Biochemistry* **30,** 8522–8529
6. Hille, R., and Anderson, R. F. (1991) *J. Biol. Chem.* **266,** 5608–5615
7. Rohlfs, R. J., and Hille, R. (1991) *J. Biol. Chem.* **266,** 15244–15252
8. Rohlfs, R. J., Huang, L., and Hille, R. (1995) *J. Biol. Chem.* **270,** 22196–22207
9. Anderson, R. F., Jang, M.-H., and Hille, R. (2000) *J. Biol. Chem.* **275,** 30781–30786
10. Hille, R. (1996) *Chem. Rev.* **96,** 2757–2816
11. Olson, J. S., Ballou, D. P., Palmer, G., and Massey, V. (1974) *J. Biol. Chem.* **249,** 4363–4382
12. Porras, A. G., and Palmer, G. (1982) *J. Biol. Chem.* **257,** 11617–11626
13. Enroth, C., Eger, B. T., Okamoto, K., Nishino, T., Nishino, T., and Pai, E. F. (2000) *Proc. Natl. Acad. Sci. U. S. A.* **97,** 10723–10728
14. Dobbek, H., Gremer, L., Meyer, O., and Huber, R. (1999) *Proc. Natl. Acad. Sci. U. S. A.* **96,** 8884–8889
15. Palmer, G., and Massey, V. (1969) *J. Biol. Chem.* **244,** 2614–2620
16. Stiefel, E. I. (1977) *Proc. Natl. Acad. Sci. U. S. A.* **70,** 988–992
17. Stiefel, E. I. (1977) *Prog. Inorg. Chem.* **21,** 1–221
18. Bordas, J., Bray, R. C., Garner, C. D., Gutteridge, S., and Hasnain, S. S. (1980) *Biochem. J.* **191,** 499–508
19. Cramer, S. P., Rajagopalan, K. V., and Wahl, R. (1981) *J. Am. Chem. Soc.* **102,** 7721–7727
20. Cramer, S. P., and Hille, R. (1985) *J. Am. Chem. Soc.* **107,** 8164–8169
21. Huber, R., Hof, P., Duarte, R. O., Moura, J. J. G., Moura, I., Liu, M.-Y., LeGall, J., Hille, R., Archer, M., and Romão, M. J. (1996) *Proc. Natl. Acad. Sci. U. S. A.* **93,** 8846–8851
22. Bray, R. C., and Vanngard, T. (1969) *Biochem. J.* **114,** 725–734
23. Ilich, P., and Hille, R. (1999) *J. Phys. Chem. B* **103,** 5406–5412
24. Massey, V., Brumby, P. E., Komai, H., and Palmer, G. (1969) *J. Biol. Chem.* **244,** 1682–1691

25. Kim, J. H., and Hille, R. (1993) *J. Biol. Chem.* **268,** 44–51
26. Steenkamp, D. J., and Mallinson, J.(1976) *Biochim. Biophys. Acta* **429,** 705–719
27. Kasprzak, A. A., Papas, E. J., and Steenkamp, D. J. (1983) *Biochem. J.* **211,** 15870–15876
28. Gutfreund, H. (1977) *Enzymes: Physical Principles*, p. 173, John Wiley & Sons, New York
29. Schuler, R. H., Patterson, L. K., and Janata, E. (1980) *J. Phys. Chem.* **84,** 2088–2091
30. Mulazzani, Q. G., D'Angelantonin, M., Venturi, M., Hoffman, M. Z., and Rodgers, M. A. J. (1986) *J. Phys. Chem.* **90,** 5347–5352
31. Anderson, R. F., and Patel, K. B. (1984) *J. Chem. Soc. Faraday Trans. I* **80,** 2693–2702
32. Lim, L. W., Shamala, N., Mathews, F. S., Steenkamp, D. J., Hamlin, R., and Xuong, N. (1986) *J. Biol. Chem.* **261,** 15140–15146
33. Wilson, E. K., Huang, L., Sutcliffe, M. J., Mathews, F. S., Hille, R., and Scrutton, N. S. (1997) *Biochemistry* **36,** 41–48
34. Romão, M. J., Archer, M., Moura, I., Moura, J. J. G., LeGall, J., Engh, R., Schneider, M., Hof, P., and Huber, R. (1995) *Science* **270,** 1170–1176
35. Hille, R., Hagen, W. R., and Dunham, W. R. (1985) *J. Biol. Chem.* **260,** 10569–10575
36. Pace, N., and Stankovich, M. (1991) *Arch. Biochem. Biophys.* **287,** 97–104
37. Lowe, D. J., Lynden-Bell, R. M., and Bray, R. C. (1972) *Biochem. J.* **130,** 239–249
38. Lowe, D. J., and Bray, R. C. (1978) *Biochem. J.* **169,** 471–479
39. Gremer, L., Kellner, S., Dobbek, H., Huber, R., and Meyer, O. (2000) *J. Biol. Chem.* **275,** 1864–1872
40. Caldeira, J., Belle, V., Asso, M., Guigliarelli, B., Moura, I., Moura, J., and Bertrand, P. (2000) *Biochemistry* **39,** 2700–2707
41. Iwasaki, T., Okamoto, K., Nishino, T., Mizushima, J., Hori, H., and Nishino, T. (2000) *J. Biochem.* (*Tokyo*) **127,** 771–778
42. Marcus, R. A. (1965) *J. Chem. Phys.* **43,** 679–701
43. Marcus, R. A., and Sutin, N. (1985) *Biochim. Biophys. Acta* **811,** 265–322
44. Moser, C. C., Page, C. C., Farid, R., and Dutton, P. L. (1995) *J. Bioenerget. Biomembr.* **27,** 263–274
45. Moser, C. C., Page, C. C., Chen, X., and Dutton, P. L. (2000) in *Subcellular Biochemistry. Vol. 35: Enzyme-Catalyzed Electron and Radical Transfer* (Holzenburg, A., and Scrutton, N. S., eds) pp. 1–28, Kluwer Academic/ Plenum Publishers, New York
46. Jones, R. M., Inscore, F. E., Hille, R., and Kirk, M. L. (1999) *Inorg. Chem.* **38,** 4963–4970
47. Cammack, R., Barber, M. J., and Bray, R. C. (1976) *Biochem. J.* **157,** 469–478
48. Hille, R., Fee, J. A., and Massey, V. (1981) *J. Biol. Chem.* **257,** 8933–8940
49. Volbeda, A., Charon, M.-H., Piras, C., Hatchikian, E. C., Frey, M., and Fontecilla-Camps, J. C. (1995) *Nature* **373,** 580–587
50. Rousset, M., Montet, Y., Guigliarelli, B., Gorget, N., Asso, M., Bertrand, P., Fontecilla-Camps, J. C., and Hatchikian, E. C. (1998) *Proc. Natl. Acad. Sci. U. S. A.* **95,** 11625–11630
51. Pershad, H. R., Duff, J. L. C., Heering, H. A., Duin, E. C., Albracht, S. P. J., and Armstrong, F. A. (1999) *Biochemistry* **38,** 8992–8999
52. Anderson, R. F., Schopfer, L. M., and Massey, V. (1987) in *Flavins and Flavoproteins, Proceedings of the 9th International Symposium* (McCormick, D. B., and Edmondson, D. E., eds) pp. 279–282, Walter de Gruyter & Co., Berlin
53. Thauer, R. K., Klein, A. R., and Hartmann, G. C. (1996) *Chem. Rev.* **96,** 3031–3042